REPORT DOCUMENTATION PAGE

AFRL-SR-BL-TR-98-
0616

1. AGENCY USE ONLY (Leave Blank)	2. REPORT DATE	3. REPORT TYPE AND DATES COVERED
	8-30-98	Final 6-1-97 to 5-31-98

4. TITLE AND SUBTITLE
MODE-LOCKED SEMICONDUCTOR LASER AT 0.2 mm (1.5 THz)

5. FUNDING NUMBERS
G
F49620-97-1-0434

6. AUTHORS
ROBERT E. PEALE

7. PERFORMING ORGANIZATION NAME(S) AND ADDRESS(ES)
UNIVERSITY OF CENTRAL FLORIDA
ORLANDO 32816

8. PERFORMING ORGANIZATION REPORT NUMBER
1168506

9. SPONSORING / MONITORING AGENCY NAME(S) AND ADDRESS(ES)
BMDO / AFOSR
(Alan Craig)
AFOSR/PKC
110 Duncan Ave Room B115
Bolling AFB DC 20332-8050

10. SPONSORING / MONITORING AGENCY REPORT NUMBER

11. SUPPLEMENTARY NOTES

12a. DISTRIBUTION / AVAILABILITY STATEMENT

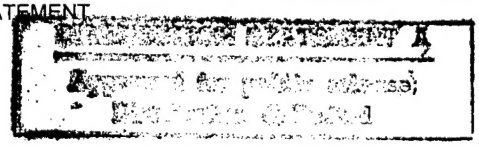

12b. DISTRIBUTION CODE

13. ABSTRACT *(Maximum 200 words)*

Pulse separation control for mode-locked far-infrared p-Ge lasers, self-mode-loching in p-Ge laser emission, and high-field Stark effect for shallow impurity lines in p-Ge laser emission are reported.

14. SUBJECT TERMS	15. NUMBER OF PAGES
THz, sub millimeter, far infrared, laser, mode locked, semiconductor, germanium	18
	16. PRICE CODE

17. SECURITY CLASSIFICATION OF REPORT	18. SECURITY CLASSIFICATION OF THIS PAGE	19. SECURITY CLASSIFICATION OF ABSTRACT	20. LIMITATION OF ABSTRACT

Mode-locked Semiconductor Laser at 0.2 mm (1.5 THz)
Final Technical Report
BMDO/AFOSR-DURIP F49620-97-1-0434

Robert E. Peale
Department of Physics, CREOL and EE
University of Central Florida
Orlando, FL 32816
rep@physics.ucf.edu

A fast transient digitizer (Tektronix SCD5000) was purchased with this equipment grant for time domain detection of mode-locking in p-Ge lasers. A list of publications which acknowledge this award is given at the end of this report together with a list of the participants in the research.

The three main discoveries made with the assitance of this award are described in the following abstracts and then again in more technical detail. The first is the subject of a patent disclosure.

Pulse separation control for mode-locked far-infrared p-Ge lasers

Active mode locking of the far-infrared p-Ge laser giving a train of 200 ps pulses is achieved via gain modulation by applying an rf electric field together with an additional bias at one end of the crystal parallel to the Voigt-configured magnetic field. Harmonic mode locking yields a train of pulse pairs with variable time separation from zero to half the roundtrip period, where pulse separation is electrically controlled by the external bias to the rf field. Potential applications include telemetry via pulse separation modulation.

Self-mode-locking in p-Ge laser emission

Investigations of the dynamics of the far-infrared p-Ge laser emission reveal strong periodic soliton-like intensity spikes with less than 100 ps duration. We interpret these spikes as self-mode-locking of p-Ge laser modes. The effect becomes more pronounced when a GaAs/AlGaAs/InGaAs quantum well structure on a semi-insulating GaAs substrate is inserted into the laser cavity.

High-field Stark Effect for shallow impurity lines in p-Ge laser emission

High resolution spectra of the far-infrared intravalenceband Ge:Ga laser, operating in crossed electric and magnetic fields, have been measured by gated Fourier spectroscopy in the low frequency range 50-60 cm^{-1} near the G absorption line of the Ga impurity. The 0.04 cm^{-1} resolution was sufficient to resolve the longitudinal mode structure of the laser and spectral shifts that depend on applied fields. These shifts provide information on the high-field Stark effect for shallow impurity levels in Ge.

TECHNICAL DETAILS

I. Pulse separation control for mode-locked far-infrared p-Ge lasers

Harmonic active mode locking was found for the first time with important new observations concerning electrical control of gain modulation and pulse separation. Far-infrared p-Ge lasers operate in a wavelength range from 70 to 200 μm. Usual p-Ge lasers generate far-infrared pulses with a few μs duration and peak power of 1 to 10 Watt. Stimulated emission occurs on direct optical transitions between light- and heavy-hole valence subbands in bulk p-Ge at liquid helium temperatures in strong crossed electric and magnetic fields. Population inversion is built up at certain ratios E/B, when heavy holes repeatedly emit an optical phonon after being accelerated beyond the threshold energy (37 meV), while light holes move on closed cyclotron orbits below this threshold and have a much longer lifetime. Due to their wide spectrum these lasers are promising for generation of short (picosecond) pulses of THz radiation by means of active or passive mode-locking for time-resolved (linear and non-linear) THz spectroscopy and other related applications.

During this grant period, 200 ps pulses of p-Ge laser radiation were obtained by active mode locking with gain modulation at one end of the laser crystal, with the modulation frequency (ν_{rf}) equal to half the cavity roundtrip frequency (ν_{RT}). The rf field is applied parallel to the magnetic field, and periodically accelerates light holes beyond the optical phonon threshold, upon which they are predominantly scattered to the heavy hole band. As a consequence, the gain is modulated at the roundtrip frequency (twice per rf period), inducing mode locking.

More surprising results were obtained when active mode locking was demonstrated for a laser crystal with $\nu_{RT} = \nu_{rf}$ and with an rf apparatus having the additional possibility of an electric bias to the rf field. This bias allowed us to control the characteristics of gain modulation and of the resulting mode-locked pulses. With this set-up, generation of two pulses per round trip (harmonic mode locking) was achieved for the first time, and electrical control of the time delay between the pulses was demonstrated.

Single-crystal, Ga-doped, p-Ge with a concentration of 7×10^{13} cm^{-3} was cut into a rectangular bar with a cross section of 5×7 mm^2 and a length of 84.2 mm. Ohmic contacts were made by Al-evaporation and subsequent annealing at opposite lateral sides of the crystal ($5 \times L$ mm^2), and then covered with In. The crystal ends were polished parallel to each other within 1' accuracy and two external copper mirrors were attached to them via 20 μm teflon film (Fig. 1). Crystals were immersed in liquid helium at 4 K. Magnetic fields up to 1.4 T were applied in Voigt geometry using a room temperature electromagnet (Walker Scientific HF-9H) external to the cryostat (Janis 8DT). Electric field pulses E_{HV} are applied from a low duty-cycle thyratron pulser. The field orientations were $E_{HV} \parallel [1\text{-}1\ 0]$ and $B \parallel [112]$. Radiation was conducted out of the top of the cryostat using a brass light pipe sealed with a teflon lens. For local regulation of the

orientation and fast modulation of E_{HV}, small additional contacts with a length of ~4 mm were placed perpendicular to the main contacts at one end of the crystal (Fig.1) for providing an additional electric field $E_L \parallel B$. In this way, the orientation of E_{HV} can be regulated (by changing the bias) and/or modulated (by applying rf power) at one end of the laser crystal ($E_{rf} \parallel B$), which provides the gain modulation for active mode-locking. By choosing a crystal length of 84.2 mm, the rf frequency ν_{rf} near 452 MHz of relatively cheap ham-radio electronics can be used, such that the cavity roundtrip frequency $\nu_{RT} = \nu_{rf}$. Since the impedance of the crystal between the rf contacts is low, high rf power is required, in part to overcome the unavoidable imperfect impedance match to the dynamic load. The rf system assembled for the experiments produces clean sub-μs pulses which just overlap the HV pulses to prevent heating of the laser crystal by the rf. Fig.2(a) presents a schematic of the rf circuit and intermediate output. The General Radio 1362 UHF oscillator delivers about 0.3 W CW signal that is frequency stable within a few tens of kHz. A directional coupler feeds a fraction of this signal to a Stanford Model SR620 frequency counter. The main part goes to a Minicircuits Model 15542 PIN diode switch controlled by 8 V signals from a home built controller, that itself is driven by standard TTL pulses. The (attenuated) signal after the switch is plotted in Fig.2(b) to demonstrate the sharp rise and fall and the short pulse lengths obtainable. From the switch, low duty-cycle rf bursts enter a GE MASTR II solid-state power amplifier with gain control to give up to 40 W. This is fed to a Henry Radio Model 2004A tube amp to give up to 800 W. A Microwave Devices 318N3 directional coupler and HP 420A crystal detectors monitor forward and reflected rf power. Power measurements were verified by direct observation of the rf voltage on a fast oscilloscope. Simple isolation capacitors were used to improve impedance match to the dynamic load and protect HV and rf systems from each other. The additional bias to the rf signal is supplied by dividing the potentials U1 and U2 directly from the main high voltage pulse using two variable resistors.

Time domain detection of the laser output used a whisker-contacted Schottky-diode detector. The diode chip (1T17(82)) was purchased from the University of Virginia and the corner cube was made by Savant-Vincent, Inc., Tampa, FL. Whiskers were formed, electrolytically sharpened, and contacted to the diode by the authors. The detector was biased using a simple homemade battery powered current source and a Minicircuits 15542 bias-T. A Picosecond Pulse Labs 5840 amplifier with 10 GHz bandwidth boosted signals, which were then recorded on a Tektronix SCD5000 transient digitizer with 4.5 GHz analog bandwidth, 200 G-samples/s,and 11 bits vertical resolution (2 mV quantization steps).

Fig.3 shows the output of the actively mode-locked laser for different settings of the external bias (U1-U2). The cavity roundtrip time of our 84.2 mm long sample is calculated to be 2.20 ns giving a roundtrip frequency of $\nu_{RT} = 453.6$ MHz. Experimentally, a resonance is found at 453.8 MHz, where the applied rf is unable to extinguish lasing, indicating mode locking. Apparently, a small change in the additional bias to the rf modulation field now has a significant

influence on the output of the mode-locked laser, which is now periodic at the roundtrip frequency. Increasing the offset causes the mode-locked pulses to broaden and eventually split into two. Further bias increase causes further separation of the pulses within each pair. This behavior is explained in Fig.4, which shows a schematic of gain modulation and the resulting pulse train due to an rf field for three different rf offsets. In each subfigure, the upper left curve shows the decrease of gain due to small E_L field along the magnetic field direction. The upper right curve shows the gain modulation that results from the biased rf signal shown in the lower left corner, while the lower right bold curve shows the expected output pulse train. When E_L (i.e. the voltage U1-U2 in Fig.2(a) between the additional contacts is applied at the peak of the gain-versus- E_L curve (Fig.4(c)), gain modulation occurs at twice the rf frequency, and the double pulse output from harmonic mode locking is expected. Moving the bias away from the point of maximum gain, the gain is more and more modulated at the single rf frequency, and the pulses in each pair move toward each other (Fig.4(b)), until they are completely merged and a train of single pulses is generated (Fig.4(a)). A comparison of Figs.3 and 4 shows that the experimentally observed output without any external biasing is connected to a situation where the rf modulation is already offset from the top of the gain-vs.- EL curve (Fig.4(a)), and external biasing is neccesary to bring the rf modulation to the top of this curve (Fig.4(c)). The 'intrinsic' voltage offset can be shown to be due to charging of the laser crystal because of anisotropy of the hot hole distribution in k-space. For the same reason as here, external biasing was shown to enable optimization of the gain for the normal microsecond-pulse operation (without rf), and significant improvement of the output of an actively mode-locked p-Ge laser with $\nu_{rf} = \nu_{RT}/2$. Upon moving to the top of the gain-vs.- E_L curve, the total gain is optimized in the first case, while in the second the optimal situation for mode locking at twice the rf frequency is reached.

The assumption of an 'intrinsic E_L field' is confirmed by studying the influence of bias change on pulsed (quasi-CW) operation of the laser. Fig. 5 shows the region of observed lasing in U2,U1 parameter space. The difference U2-U1 is a direct measure of the E_L field due to charging in the region between the rf contacts, and the zero of this field should roughly correspond to U1 = U2, although there might be a small offset caused by misalignment of the rf contacts. The width of this region confirms the strong dependence of the gain on E_L: changing U2 - U1 over ±50V (E_L ~100 V/cm) from its optimum value brings the laser below threshold. The open circle in Fig. 5a indicates the values of U2,U1 that the laser establishes by itself without external biasing. It appears at the border of the lasing region, again indicating that there is an intrinsic field $E_L \neq 0$ which has already significantly reduced the gain. By applying an external bias, this E_L field can be compensated and the gain in the region between the additional contacts is electrically optimized, yielding longer laser pulses of higher intensity. In Fig. 5b, both the 'intrinsic' and the gain-optimized values of U2-U1 are plotted when the laser crystal is rotated around its long axis. The difference ranges from about 30 V/cm for $\alpha = -2°$ to zero at $\alpha = 2°$.

As a starting point for a theoretical discussion of these effects, we note that a net intrinsic E_L field as observed here can only occur for situations with limited symmetry along the magnetic field, and the field orientation $\mathbf{E}_{HV} \parallel [1\text{-}10]$ and $\mathbf{B} \parallel [112]$ used in our active-mode-locking experiments indeed lacks a symmetry plane perpendicular to **B**. Monte Carlo simulations show that for such orientations a significant current component $\mathbf{j}_L \parallel \mathbf{B}$ might occur even in perfectly crossed **E** and **B** fields. For streaming holes, this is caused by the highly anisotropic, elongated hole distribution in the anisotropic band (similar to well-known Sasaki-Shibuya effect), while for accumulated holes it results from asymmetry of the accumulation region.

The Monte Carlo result in Fig. 6b shows that j_L (normalized by the total current j) changes heavily when the electric field is rotated in a plane perpendicular to the magnetic field. Fig. 6a shows the calculated electric field distribution perpendicular to **B** for our 42 mm laser crystal in Voigt configuration. Current saturation is implemented by taking σ_T proportional to E^{-f}. Near the long ends of the laser rod, the total electric field $E_{tot}=(E_{HV}^2+E_{Hall}^2)^{1/2}$ is larger and rotated over an angle ϕ with respect to the applied field $\mathbf{E}_{HV}$ due to the usual Hall effect. Space-charge effects significantly enlarge the affected area. Combining both pictures, one concludes that, due to the inhomogeneity of E_{tot}, the E_L field is relatively small in the central part of the sample, but quite strong in the area near its long-ends (the region between the additional contacts). In Fig. 6c the current j_L in the latter region is plotted as a function of the additional E_L field along the magnetic field. For a crystal mounted perpendicular to **B** (i.e not tilted, $\alpha = 0°$), j_L has to be zero, and an internal E_L field will be established by charging to meet this requirement (and since for a Voigt-configured sample the dimensions parallel to **B** are relatively small, this field extends throughout the whole cross-section). In Fig. 6c, j_L for the total hole distribution is zero for about 30 V/cm. This corresponds very nicely with the experimentally observed offset of U2-U1 = 15 V over 5 mm in Fig. 5b at $\alpha=0°$. The offset is expected to be zero for $j_L/j = E_L/E = \sin\alpha$, and in Fig. 6c this occurs for $\alpha \sim 2°$, again in good agreement with the experimental value. Only for this value of α, no external bias is needed to optimize the gain or move the zero of the rf field to the top of the gain-vs.-E_L curve in order to have gain modulation at twice the rf frequency (Fig. 4c). Early experiments (with only modest rf power) found a rf resonance when the crystal was tilted about 2 degrees. Finally, the Monte Carlo simulations show that the offset shifts about 10 V/cm as the crystal is heated from 4.2 K to about 20 K during the macropulse. This might lead to a strong pulse broadening when the gain is modulated at twice the rf frequency, as the situation moves from Fig. 4a to Fig. 4b during the macropulse.

To summarize, active mode-locking of the p-Ge far-infrared laser with $\nu_{rf} = \nu_{RT}$ results in the generation of an output train of double far-infrared pulses with < 200 ps duration (harmonic

mode locking). By changing the external bias to the rf modulation field the temporal separation for a pair of mode-locked pulses can be controlled. The ability to generate a train of double pulses with electrically controllable pulse separation suggests that mode-locked p-Ge lasers may have promise for telemetry in special applications.

II. Self-mode-locking in p-Ge laser emission

Fig. 7 shows the laser operating zone of applied E and B fields, which splits into low and high field regions. These correspond to low and high frequency laser emission, respectively. Without active mode locking, the laser still might have a strongly varying intensity, periodic with the roundtrip time of the laser cavity, which results from modes being accidentally in phase to some extent. For the low frequency part of the laser spectrum, which is split in several discrete lines containing only 10 to 20 longitudinal modes, such coincidences are likely, especially in the rising edge of the laser pulse. In the high frequency part of the spectrum, hundreds of modes oscillate simultaneously with random phases, and a sharply peaked temporal structure due to some coincidental phase relation is much more unlikely. We found the first evidence for self-mode-locking in the high frequency region of the p-Ge laser. It appears as a clear nonlinear effect at the peaks of a slowly oscillating laser intensity. As a result, a train of radiation spikes shorter than 100 ps is generated without active gain modulation or added passive elements. The short spikes usually appear at the rise of the slow intensity oscillations, and disappear when the background intensity falls.

The active Ge crystal studied here has dimensions 4.5 x 7.3 x 28.0 mm^3. The magnetic field is applied along [1-10] in Faraday geometry. The laser radiation propagates along the long crystal axis [1-1 0]. Spectroscopy was performed with a research grade FTIR (Bomem DA8)using "Event-locked" gated-acquisition electronics(Zaubertek).

The p-Ge laser spectrum without intracavity frequency selection is 15-30 cm^{-1} broad and tunable between 50 and 140 cm^{-1} by changing the applied fields. In the high-frequency region (Fig. 7), this spectrum can contain a few hundred longitudinal laser modes, but in the low-frequency region below 70 cm^{-1}, the spectrum is split up in discrete lines related to shallow impurity transitions. The broadest of the low frequency laser emission lines is shown in Fig. 8. This is the first broadband spectral measurement of p-Ge laser output with resolution high enough to resolve the longitudinal mode structure. The observed equidistant mode spacing $\Delta\nu$ in Fig. 8 is related to the longitudinal round-trip time τ by $\Delta\nu = 1/\tau = c / (2nL) = 1363$ MHz, or $\tau = 734$ ps, where L is the active crystal length, and n =3.925 is the refractive index. The corresponding mode beating pattern could easily display strong oscillations of the laser intensity at the round trip frequency $\Delta\nu$, simply by having the phases of each mode accidentally similar. In the high field region, however, such coincidences and strong oscillations are much less likely.

Fig. 9 shows digitally captured traces of the output intensity of this particular crystal at three different time scales. The output intensity is strongly modulated at about 44 MHz (Fig. 9a). These oscillations are much slower than the cavity round trip frequency of 1363 MHz. At a higher temporal resolution, trains of very sharp spikes are found on the maxima of the slow intensity oscillations (Fig. 9b). Such spikes are absent from the 44 MHz valleys and they start to grow rapidly as the intensity increases. The round trip time for the sharp spikes is 722 ps, which is close to the calculated cavity round trip time of 734 ps. We take the occurrence of the sharp spikes to be evidence for self-mode-locking. Fig. 9(c) and (d) show close-ups of portions of the trace in Fig. 9b. Sampled data points are indicated by circles. The unevenness in the rise of self-mode-locking in Fig. 9c is clearly a sampling effect. The points are separated by 50 ps, showing that the self-mode-locked pulses have a width less than the 80 ps rise time allowed by the bandwidth of the electronics. These are the shortest pulses yet observed from p-Ge lasers

Additionally, we have investigated the temporal behavior of emitted radiation from this p-Ge laser when a GaAs/AlGaAs/InGaAs quantum well structure on a semi-insulating GaAs substrate with a thickness of 0.5 mm and parallel polished surfaces is inserted into the cavity between the active crystal and the back mirror. The short radiation spikes become much more pronounced and repeatable. This is shown in Fig. 10. The inset shows another shot at a finer timescale. The quantum well structure consists of 40 nm n^+ GaAs ($n>10^{18}\,cm^{-3}$), 40 nm n^+ $Al_{0.24}\,Ga_{0.76}\,As$ ($n>10^{18}\,cm^{-3}$) 15 nm i-$In_{0.18}\,Ga_{0.82}\,As$, and 100 nm i-GaAs layers on top of a GaAs substrate.

These experiments demonstrate self-generation of intense spikes as short as 80 ps in the far-infrared p-Ge laser, which is shorter than obtained so far by active mode locking. We take this result as tentative evidence for self-mode-locking. Strong slow intensity oscillations seem to provide the conditions for build-up of these spikes. The experimental data are not yet conclusive with respect to the origin of either the slow oscillations or the short pulse formation. Various possibilities are discussed here briefly.

The most straightforward explanation for the 44 MHz oscillation is beating of transverse modes. The observed synchronization of spike generation to the rise in intensity might, however, suggest that actual modulation of the gain occurs at this low frequency, and peaks grow during a period of net gain and disappear when losses are dominant. The observed train of spikes corresponds to the formation of a soliton-like electromagnetic pulse traveling in the laser cavity due to nonlinear processes in the active medium. Since the active p-Ge laser crystal is a hot carrier system interacting with a high-intensity radiative field, operating in a strongly nonlinear regime in many aspects, several possible mechanisms can be suggested for self-mode-locking. First of all, the population inversion in part of the crystal might be destroyed due to the inhomogeneity of doping and/or inhomogeneity of the applied electric field. This part could then act as a saturable absorber causing passive mode locking. The observed enhancement upon including a nonlinearly absorbing spacer into the cavity seems to support such an interpretation. However, the observed rapid rise in spike intensity remains somewhat surprising, considering the supposed low gain of

the medium, and this might suggest other mechanisms such as soliton mode-locking due to nonlinear changes of the refractive index. Unfortunately, the magnitude of these index changes in p-Ge laser systems has been little studied so far, although the suggested strongly nonlinear birefringence caused by Faraday rotation and slightly different index for higher-order transverse modes, might turn out to be important factors for the generation of temporal or spatial optical solitons, respectively, in ways similar to pulse formation in fiber laser systems. Clearly, further experimental and theoretical studies are necessary to clarify this issue.

The passive way of obtaining picosecond far-infrared pulses from a p-Ge laser is much simpler than the active mode-locking scheme, which involves high-power, ultra-high-frequency rf techniques. A disadvantage of self-mode-locking is the rather large background output intensity (about 40-50 %) observed in Figs. 9 and 10, which is suppressed when the laser is actively mode-locked with a sufficiently strong rf field. However, to the extent that this background is due to unlocked, or spatially separated (internal-reflection) modes, it can possibly be removed by bringing these modes below threshold with an optimized resonator design. Also, hybrid mode-locking schemes, where active and passive mode locking are combined, could yield the advantages of both schemes: short pulses with low jitter and background. The rapid rise in pulse intensity suggests that pulse amplitude modulation telemetry with a mode-locked pulse train of THz laser radiation may be possible, although it remains unclear how to control such modulation. Potential applications might include secure, local area communication by free THz beams or longer range communication in space.

III. High-field Stark Effect for shallow impurity lines in p-Ge laser emission

p-Ge laser spectra are split into discrete spectral lines in the region of shallow acceptor transitions, so that the laser spectrum looks similar to the spectrum of p-Ge photoconductivity. For the Ga-doped laser the discrete spectral structure occurs in the so-called low-frequency region (50 - 60 cm^{-1}) near the G absorption line of the Ga impurity. This effect occurs even though the dopant centers are presumably impact-ionized in a strong electric field. The role of impurity absorption transitions in p-Ge laser spectra remains unclear, partly because of the lack of high resolution experimental spectral data.

We measured the highest resolution spectra of the low-frequency region of the p-Ge laser to date. Our resolution was 0.04 cm^{-1} (1 GHz). Heterodyne spectroscopy allows much better resolution (MHz), but only over a narrowband range of a few GHz.

The active sample used in the experiments was 5 x 7 x 27.9 mm^3. The laser is inserted into a superconductive solenoid, so that the magnetic field is applied along the long sample axis [1-10] (Faraday geometry). The whole system is immersed in liquid helium in an optical cryostat with 4K ZnSe and room temperature polyethylene windows. The radiation passes through the spectrometer and is detected by a far-infrared Si bolometer (InfraRedLabs) with a 100 cm^{-1} low-pass filter.

The evolution of the p-Ge laser spectrum versus applied fields is shown in Fig. 11. The spectrum consists of three separate bands of stimulated emission nearly symmetrically arranged around the zero-field Ga absorption G-line, marked in Fig. 11 by the dashed line. The fine periodic structure of the spectra within each band is caused by longitudinal modes of the laser cavity, which has a mode distance of 1368 MHz. These bands shift to lower frequencies upon increasing applied fields from E~ 0.51 kV/cm, B~ 0.35T to E ~ 0.76 kV/cm, B~0.59 T. The shift is 0.3-0.4 cm^{-1} for the sharp central band at 54.7 cm^{-1} and 0.6-0.8 cm^{-1} for the high-frequency-side satellite band at 57.0-57.5 cm^{-1}. These shifts are related to Stark and Zeeman effects of shallow impurity transition lines, and this is one more confirmation that the discrete structure of the p-Ge laser spectrum is related to impurity transitions. Note that under ordinary experimental conditions, when the p-Ge sample is outside the laser cavity, measurements of the Stark effect in such high electric fields are difficult because shallow impurities are almost completely ionized due to impact ionization. For an adequate interpretation of the observed effects, theoretical work is needed to predict impurity level positions and splitting when large electric and magnetic fields are applied simultaneously.

In summary, these measurements suggest a way to investigate the high-field Stark effect for shallow impurities even in the presence of complete electrical breakdown. Such experimental information can provide a sensitive test of the effective mass theory for shallow acceptors in strong fields[1].

Reference

1. W. Kohn, in Vol.5 of Solid State Physics, edited by F. Seitz and D. Turnbull (Academic Press, New York, 1957), p. 311.

FIGURES

Fig. 1. Diagram of p-Ge laser crystal with contacts, end mirrors, applied fields, and rf electric field modulation at one end.

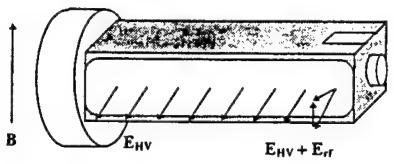

Fig. 2. (a) Rf setup. Thick lines denote coaxial lines.(b) Example of (attenuated) output of the pulse-forming switch.

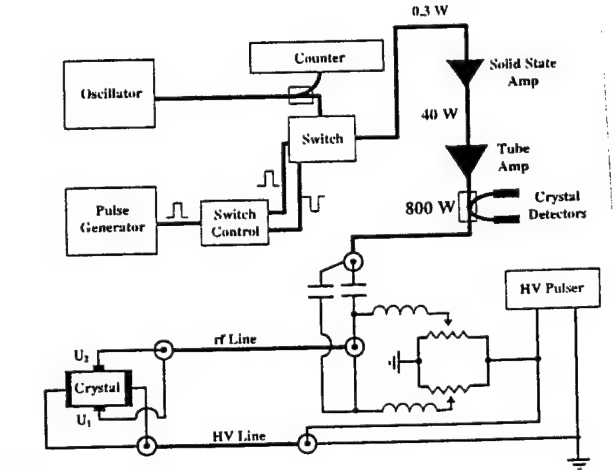

(a)

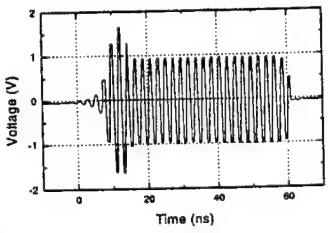

(b)

Fig. 3. Mode-locked p-Ge laser pulse structure for the 84.2 mm crystal. External bias added to the rf modulationincreases from zero in the three frames from top to bottom.

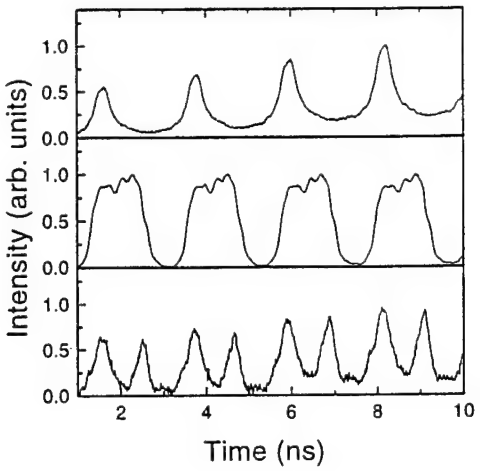

Fig. 4. Explanation of bias effects and pulse-separation control. The left curve plots gain versus external bias. The right curveshows the modulation of the gain versus time, when the rf fieldis applied at the bias level indicated. The pulse train expected to result is also indicated. The three situations(a) large offset: modulation far from peak of gain-vs.- E_L ,(b) small offset: modulation close to peak of gain-vs.- E_L curve,and (c) zero offset: modulation at peak of gain-vs.- E_L curve mimic the experimental results in Fig. 3.

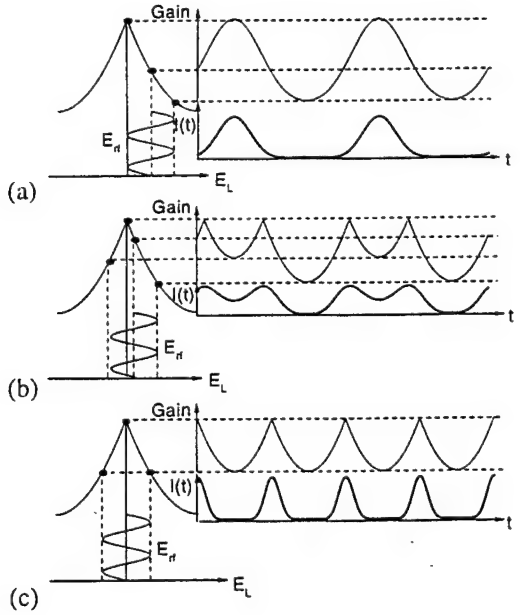

Fig. 5. (a) Lasing domain in U_1, U_2 space. The open circle indicates the operating point without the bias-forming circuit. (b) Potential U_2-U_1 on rf contacts when laser is rotated around its long axis, thereby introducing a nonorthogonality $\Delta\alpha$ between **E** and **B**. The solid symbols denote the value without bias-forming circuit, while the open triangles indicate the setting with strongest lasing.

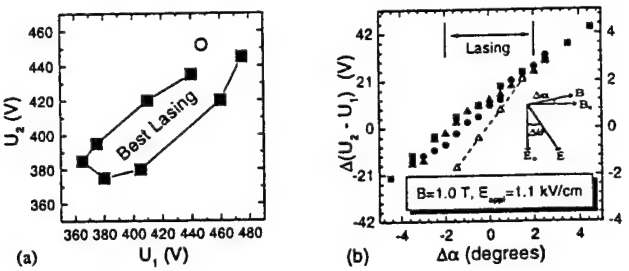

Fig. 6. Equipotential lines (each 100 V) in the sample cross-section perpendicular to the magnetic field for f=0 (no space-charge, dash-dotted lines) and f=0.7 (solid lines). The dotted lines indicate contour lines of the space charge (in units of ε times 10^6 Vm^{-2}) formed for f=0.7. The distance d between the contacts is 7 mm, while the length l of the contacts is 42 mm. A constant Hall-angle α_H=45° is assumed. (b) j_L/j versus the angle ϕ over which the electric field is rotated by the Hall effect; T=20 K, E = 1.35 kV/cm ∥ [1-10] (for ϕ=0°), B=1.0 T ∥ [112], N_I=1.3 x 10^{14} cm^{-3}, p_0=7 x 10^{14} cm^{-3}, Brooks-Herring model with self-consistent screening is used to model ionized impurity scattering. (c) j_L/j versus E_L, T=20 K, E = 1.1 kV/cm, f =-45°, B = 1.0 T ∥ [112].

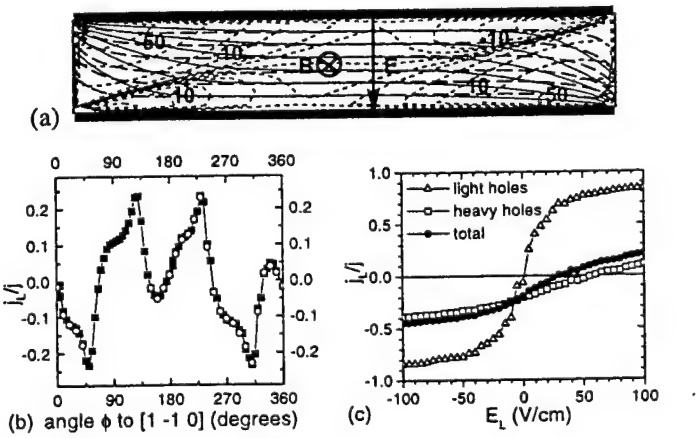

Fig. 7. Typical (E,B) field regions for low-frequency and high-frequency operation of a p-Ge laser.

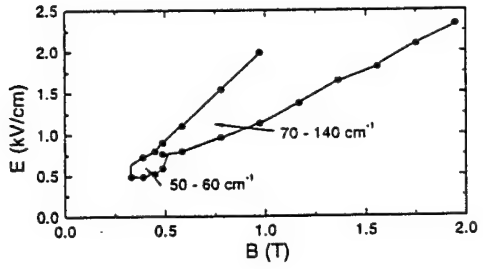

Fig. 8. Close-up of one of the spectral lines in the low-field regime showing longitudinal mode structure.

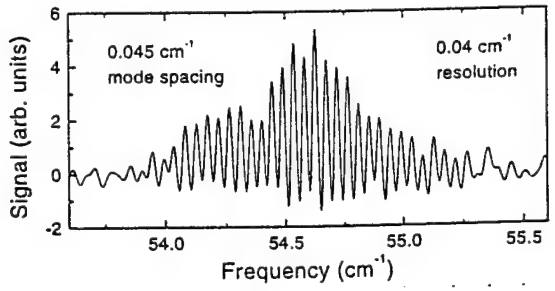

Fig. 9. (a) Laser output pulse showing 44 MHz oscillations. (b) A different shot at higher time resolution showing sharp spikes at the crests of the 44 MHz oscillations. (c) and(d) Further close-ups of (b) show that the unevenness in the peak heights is evidently a sampling fect, where points are sampled at a 50 ps interval.

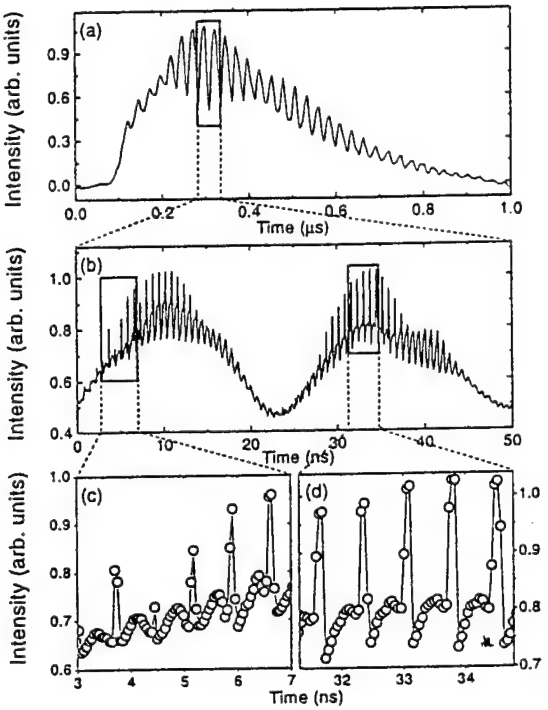

Fig. 10. Output of the self-mode-locked p-Ge laser with quantum well intracavity insert. Upon blocking the radiation, the signal drops to a baseline of about 0.05, so the peaks occur on a constant background of about equal intensity. The inset shows a different shot with higher time resolution.

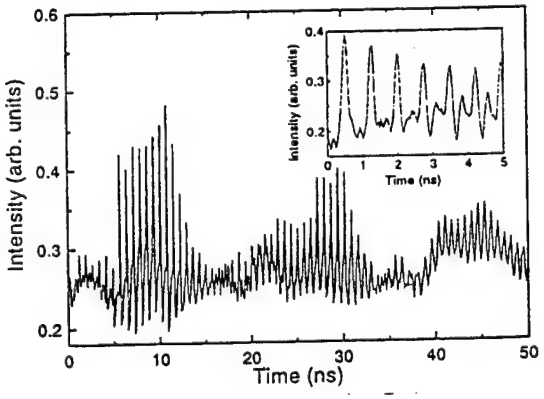

Fig. 11. p-Ge laser spectra in the low frequency band for several values of applied electric and magnetic fields. (Applied fields are defined from monitoring values as E = 0.4 kV cm^{-1}/V; B = 0.55 T/V).

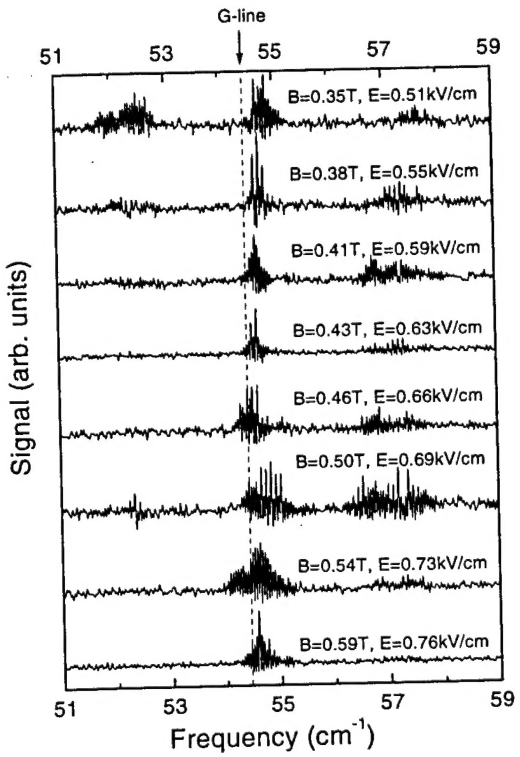

Journal publications that acknowledge this grant

1. "Evidence for self-mode-locking in p-Ge laser emission," A. V. Muravjov, R. C. Strijbos, C. J. Fredricksen, H. Weidner, W. Trimble, S. H. Withers, S. G. Pavlov, V. N. Shastin, and R. E. Peale, Submitted to Applied Physics Letters, 1 June 1998, revised version resubmitted 27 Aug 1998.

2. "Mode-locked far-infrared p-Ge laser with pulse separation control," A. V. Muravjov, R. C. Strijbos, C. J. Fredricksen, S. H. Withers, W. Trimble, S. G. Pavlov, V. N. Shastin, and R. E. Peale, submitted to Appl. Phys. Lett., 28 Aug 1998.

3. "Effect of intracavity Si etalon on p-Ge laser emission dynamics," S. H. Withers, A. V. Muravjov, R. C. Strijbos, C. J. Fredricksen, W. Trimble, S. G. Pavlov, V. N. Shastin, and R. E. Peale, 1998, in preparation.

Conference publications that acknowledge this grant

1. "Short pulse intervalence band germanium laser at sub-millimeter wavelengths," R. E. Peale, C. J. Fredricksen, W. Trimble, H. Weidner, A. Jamison, R. C. Strijbos, A. V. Muravjov, S. G. Pavlov, and V. N. Shastin, in Technical digest of Workshop on Radiative Processes and Dephasing in Semiconductors, February 2-4, 1998, Coeur d'Alene, Idaho. (OSA, Wash. D.C. 1998), pp. 106-108.

2. "Fast dynamics of the p-Ge laser emission," A. V. Muravjov, R. C. Strijbos, C. J. Fredricksen, H. Weidner, W. Trimble, A. Jamison, S. G. Pavlov, V. N. Shastin, and R. E. Peale, in Conference on Lasers and Electro-Optics, OSA Technical Digest Series, pp. (Optical Society of America,Washington DC, 1998).vol. 6, pp. 132-133.

3. "Mode-locked far-infrared p-Ge laser using an offset rf electric field for gain modulation," A. V. Muravjov, R. C. Strijbos, C. J. Fredricksen, H. Weidner, W. Trimble, A. Jamison, S. G. Pavlov, V. N. Shastin, and R. E. Peale, in Radiative Processes and Dephasing in Semiconductors, edited by David Citrin (OSA, Washington DC, 1998), OSA-TOPS, vol 18, p 102.

4. "High-field Stark effect for shallow impurity lines in p-Ge laser emission," A. V. Muravjov, R. C. Strijbos, C. J. Fredricksen, H. Weidner, W. Trimble, S. H. Withers, R. E. Peale, S. G. Pavlov, and V. N. Shastin, in Proceedings of 24th International Conference on the Physics of Semiconductors, August 2-7, 1998, Jerusalem, Israel (World Scientific, Singapore, 1998) to be published.

5. "Charging effects in mode-locked Thz p-Ge lasers," R. C. Strijbos, A. V. Muravjov, C. J. Fredricksen, H. Weidner, W. Trimble, S. H. Withers, S. G. Pavlov, V. N. Shastin, and R. E. Peale, in Conference Digest of 23rd Int. Conf. on Infrared and Millimeter Waves, Sept. 7-11 1998, Essex, UK, 1998, to be published.

6. "Mode locking of far-infrared p-Ge lasers," R. C. Strijbos, A. V. Muravjov, C. J. Fredricksen, W. Trimble, S. H. Withers, S. G. Pavlov, V. N. Shastin, and R. E. Peale, in Conference Proceedings of 6th IEEE Int. Conf. on Terahertz Electronics, Sept. 3-4, 1998, Leeds, UK, 1998, to be published.

7. "Mode locking of far-infrared p-Ge lasers," R. C. Strijbos, A. V. Muravjov, C. J. Fredricksen, W. Trimble, S. H. Withers, S. G. Pavlov, V. N. Shastin, and R. E. Peale, in

Conference Digest of Workshop Middle Infrared Coherent Sources (MICS 98), Sept. 22-26, 1998, Cargese, Corsica, France, 1998, to be published.

Personnel

1. Will Trimble, high school student, set up and tested high-power pulsed rf system, participated in experiments, will attend University of Chicago in Fall.

2. Alan Jamison, high school student, built Schottky diode bias box, built computer-controlled stepper-motor magnet winder, will attend Princeton in Fall.

3. Sandra Withers, undergraduate, participated in experiments, Monte Carlo simulations, has entered UCF PhD program.

4. Chris Fredricksen, graduate student, built cryostat inserts and participated in experiments, defended MS thesis 12 June 1998.

5. Henry Weidner, graduate student, developed gated FTIR for continuously scanning interferometers, patented and commercialized it, defended PhD thesis 12/98, currently works on instrumentation development at Kennedy Space Center.

6. Remco Strijbos, post doc, responsible for fundamental concept of active mode-locking in p-Ge lasers while a graduate student in Delft, currently participates in experiments and continues with theoretical Monte Carlo simulations.

7. Andrei Muravjov, post doc, brought crystals we are using from the Institute for Microelectronics in Nizhny Novgorod, brings experience and strong direction to our activities.

8. V. N. Shastin and S. G. Pavlov, senior scientists at the Institute for Microelectronics in Nizhny Novgorod, prepared and loaned p-Ge crystals.